Available online at www.sciencedirect.com

ScienceDirect

Procedia Materials Science 4 (2014) 109 – 114

Procedia Materials Science

www.elsevier.com/locate/procedia

8th International Conference on Porous Metals and Metallic Foams, Metfoam 2013

The role of foaming agent and processing route in mechanical performance of fabricated aluminum foams

Alexandra Byakova[a,*], Iegor Kartuzov[a], Takashi Nakamura[b], Svyatoslav Gnyloskurenko[c]

[a]*Institute For Problems Of Materials Science, National Academy Of Sciences Of Ukraine , Kiev 03142, Ukraine*
[b]*Institute Of Multidisciplinary Research For Advanced Materials, Tohoku University, Sendai 980-8577, Japan*
[c]*Physical-Technological Institute Of Metals And Alloys, National Academy Of Sciences Of Ukraine, 03142, Kiev, Ukraine*

Abstract

The results of this study highlight the role of foaming agent and processing route in influencing the contamination of cell wall material by side products, which, in turn, affects the macroscopic mechanical response of closed-cell Al-foams. Several kinds of Al-foams have been produced with pure Al/Al-alloys by the Alporas like melt process, all performed with and without Ca additive and processed either with conventional TiH_2 foaming agent or $CaCO_3$ as an alternative one. Damage behavior of contaminations was believed to affect the micro-mechanism of foam deformation, favoring either plastic buckling or brittle failure of cell walls. No discrepancy between experimental values of compressive strengths for Al-foams comprising ductile cell wall constituents and those prescribed by theoretical models for closed-cell structure was found while the presence of low ductile and/or brittle eutectic domains and contaminations including particles/layers of Al_3Ti, residues of partially reacted TiH_2, Ca bearing compounds, etc. results in reducing the compressive strength to values close to or even below those of open-cell foams of the same relative density.

Peer-review under responsibility of Scientific Committee of North Carolina State University

Keywords: Al-Based Alloys; Melt Route; Processing Additives; Mechanical Properties.

* Corresponding author. Tel.: +38-044-423-8253; fax: +38-044-423-8253.
E-mail address: byakova@mail.ru

Peer-review under responsibility of Scientific Committee of North Carolina State University
doi:10.1016/j.mspro.2014.07.608

1. Introduction

Remarkable absorbing ability resulted from capacity of closed–cell aluminum foams to undergo large strains (up to 60–70%) under almost constant stress offers significant performance for crash protection and other applications where effective utilizations of impact energy is required (Ashby et al. (2000)). Particularly, Al-foam can act as an efficient impact energy absorber providing crash protection for terrestrial and marine vehicles.

A number of models based on an idealized representation of a defect-free cellular structure have been developed for interpreting mechanical behavior of ideal open- and closed-sell foams that are particularly summarized in a work by Gibson (2000). However, the actual profile of the mechanical properties for real Al-foams is far from the idealized theoretical predictions as was originally pointed out in Gibson (2000). This fact is preferably considered to arise due to mesoscopic inhomogeneity in density and other structural imperfections including cell morphology (thickness, curvature, length, etc.). Nevertheless, the microstructural aspects are still ignored in most studies, despite the known fact that microstructural features would have dramatic effects on the performance characteristics of corresponding bulk material. This problem becomes increasingly pronounced when foaming processes are performed with gas-releasing agent and other additives, resulting in unconventional matrix alloy comprising great number of various intermetallic compounds and other foreign particles. This effort is to elucidate the role of foaming agent and processing additive in influencing the mechanical performance of Al-foams processed with different kinds of parent Al-alloys via Alporas route.

2. Experiment

2.1. Materials and Experimental Procedure

Several kinds of closed-cell foams used in experimentation are listed in Table 1. Pure aluminum and several conventional Al-alloys were chosen as parent materials. All kinds of Al-foams were produced via Alporas like rout in which either titanium hydride TiH_2 or calcium carbonate $CaCO_3$ were employed as foaming agents (Byakova et al. (2006)). In addition, both hydride and carbonate Al-foams were produced either with or without Ca additive introduced into melt as thickening agent. Relative density, ρ/ρ_s, of Al-foams, which is listed in Table 2, was measured by weighing a sample of known volume. In addition, several solid alloys of compositions roughly corresponded to the cell wall materials formed in the studied Al-foams were fabricated by casting and used in experimentation. Microstructure examination of Al-foams and solid materials was done using scanning electron microscopy (SEM) in both secondary and back-scattered modes. Material elementary composition was studied using energy dispersive X-Ray spectroscopy (EDS) and electron probe microanalysis (EPMA).

Table 1. Parent alloys and processing additives used for different kind of Al-foams

Code	Parent alloy	Processing additive, wt.%
F1/F2	Al	$1TiH_2$+1Ca/$2CaCO_3$+1Ca
F3/F4	A356	$1.5TiH_2$+1Ca/$1.5TiH_2$
F5/F6	A356	$2CaCO_3$+1Ca/$2CaCO_3$
F7/F8	6061	$1.5TiH_2$+1Ca/$1.5TiH_2$
F9/F10	5356	$1.5TiH_2$+1Ca/$1.5TiH_2$
F11/F12	7075[(1)]	$1.5TiH_2$+1Ca/$1.5TiH_2$
F13/F14	7075[(1)]	$2CaCO_3$+1Ca/$2CaCO_3$

Note: [(1)] alloy was additionally doped by small amount of Sc and Zr (totally 0.6 wt.%).

2.2. Mechanical Testing

Deformation behavior of Al-foams was examined under uniaxial compressive tests performed on the prismatic specimens with a ratio of height to thickness that exceeds 1.5. The minimum dimension of the specimen in each of

three directions was seven times more than the cell size to avoid size effect. The compression tests were performed on a servo-hydraulic testing machine under displacement control and static strain rate of 1.5×10^{-3} s^{-1}.

Table 2. Characteristics for different kind of Al foams and cell wall solid materials

Code	Relative density, $(\rho/\rho_s)^{(1)}$	Solid yield strength, σ_{ys} (MPa)
F1/F2	0.37-0.21 / 0.24-0.09	42.8 ± 4.89 / 43.5 ± 7.12
F3/F4	0.17-0.30 / 0.17-0.24	220± 20.54 / 180± 21.68
F5/F6	0.18-0.29 / 0.18-0.27	195 ± 19.53 /140 ±15.67
F7/F8	0.15-0.26 / 0.25-0.43	120 ± 14.82 / 100 ± 9.85
F9/F10	0.18-0.32 / 0.31-0.40	180± 19.73 /160 ± 17.13
F11/F12	0.22-0.38 / 0.19–0.40	560± 28.24 / 540± 26.15
F13/F14	0.20-0.34 / 0.20-0.33	575±29.48 / 531 ± 15.14

Note: $^{(1)}$ ρ and ρ_s correspond to the density of foam and dense solid, respectively.

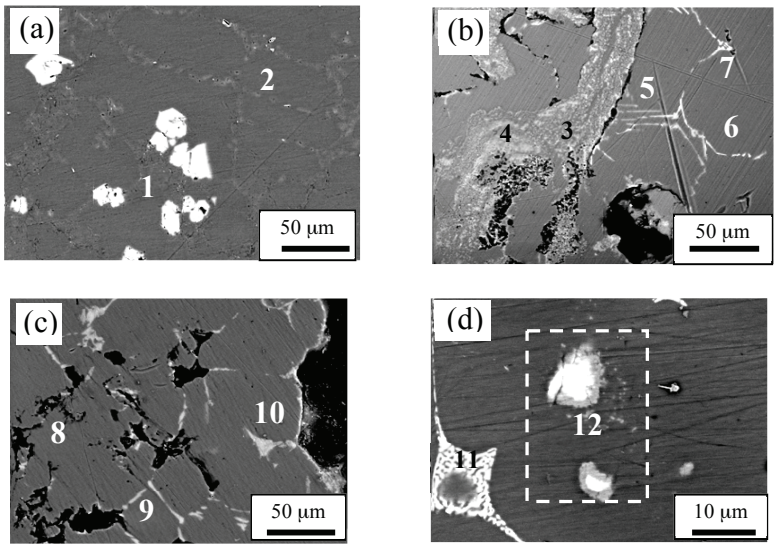

Fig. 1. SEM micrographs of cell wall materials for Al-foams such as (a) F5, (b) F7, (c) F9, (d) F12, processed either with (a) CaCO3 or with (b)-(d) TiH_2 and performed (a) – (c) with and (d) without Ca additive.

3. Results and discussion

3.1. Material Characterization

As it can be seen in Fig. 1, cell wall material for all kind of Al-foams demonstrates rather non-homogeneous microstructure consisted of coarse Al dendrites rounded by a network of eutectic domains (light grey) (Byakova et al. (2006)).

Excluding carbonate Al-foams (F2, F6, F13, and F14) cell wall materials for all another foams exhibit a lot of foreign particles. In Al foams (F3, F5) processed with Ca additive, coarse crystals compositionally corresponded to Al_2CaSi_2 intermetallic compound (1) are presented in the cell wall material besides E (Al+Si) eutectic domains (2), as can be seen in Figure 1(a). Formation of needle-shaped Al_2CaSi_2 crystals (5) is also detected in the cell wall material of Al-foam F7, as shown Figure 1 (b). Foreign particles of partly converted TiH_2 and/or its reaction products such as particles/layers Al_2Ti/Al_3Ti (12) are randomly distributed in the cell walls of hydride kinds of Al-foams (F1, F3, F4, F7-F12). In line with Byakova et al. (2006) the above Ti-rich particles are mainly presented in the cell wall material of hydride kind of Al foams (F4, F8, F10, F12) processed without Ca additive, as can be seen in Figure 1 (d). The results

of element distribution show that composition of eutectic domains formed in the cell wall material of other Al-foams was found to be rather different compared to those of parent alloys and dependent on the processing additives. Generally, dissolved Ca is largely accumulated within the eutectic domains, resulting in their local modification with formation of foreign Ca-bearing eutectic zones. In particular, besides E (α-Al + Mg_2Si) eutectic domains (6) indicative of parent alloy, foreign eutectic zones such as E (α-Al+Al_4Ca) (3), E(α-Al +Al_4CaCu) (4), and E(α-Al+Al_2CuMg) (7) are formed in Al-foam F9, as shown in Figure 1(b). The same is true for Al foam F9 for which cell wall material comprises Ca-bearing eutectic zones such as E(α-Al+Mg_2Ca) (9) and E(α-Al+Al_4Ca+Al_3Ti) (10) besides E(α-Al+Mg_5Al_8) eutectic domain (8) indicative of parent alloy, as shown in Figure 1 (c). In addition, despite of small amount (roughly about 0.26 at.%) Ti solutes in Al matrix it is also concentrated within the eutectic domains, resulting in formation Al_3Ti compound. As an example, Ti-bearing eutectic zones such as E (α-Al+Al_4Ca+Al_3Ti) (10) and E {α-Al+ T(AlCuMgZnTi)} (11) are respectively found in Al-foams F9 and F12, as shown in Figures 1 (c) and (d).

The important point concerns the difference in damage behavior of cell wall constituents comprised by different kind of Al-foams. In particular, Al+Al_4Ca eutectic domains indicative of a carbonate Al-foam (F2) demonstrate quite high plasticity that is close to α-Al dendrites, whereas cell wall constituents including eutectic domains and foreign particles/layers indicative for all another Al-foams show low ductility and/or high brittleness (Byakova et al. (2012)).

3.2. Compressive Response of Al-Foams

All kinds of Al-foams display a macroscopic mechanical response rather similar to elastic/plastic behaviour. However, different kinds of Al-foams exhibit considerable differences in microscopic deformation events "plateau" regime, as can be seen in Figs. 2 (a) and (b). In particular, carbonate Al-foam F2 with ductile Al + Al_4Ca eutectic domains in the cell wall material deform smoothly that is typical for plastic buckling (Gibson (2000)). Slight hardening/softening effects superimposed upon an increasing "plateau" stress level are seen in deformation patterns of hydride kind of Al-foams (F1, F3, F4 and F9). These deformation events are usually ascribed to the cell walls local failure being stimulated by crushing the low ductile eutectic domains and brittle foreign particles (Byakova et al. (2006)). Hydride kinds of Al-foams (F11, F12), which cell walls comprise great amount of brittle foreign particles and eutectic domains, show the most strong stress oscillations of "plateau" stress level, as can be seen in Fig. 2 (b). Moreover, compression of the above Al-foams gives undesirable high peak stress at the onset of global collapse. In addition, the presence of Ca-bearing eutectic domains in the cell wall material of Al-foam F11 results in decreases of compression strength. As it is shown in Fig. 2 (b), a remarkable improvement of mechanical behaviour is found for carbonate Al-foam (F14) with no brittle foreign particles in the cell wall material.

3.3. Comparison of Al-foam Compressive Strength with Theoretical Models

Comparison of the experimental results of this study with the theoretical predictions was fulfilled to estimate the role of cell wall microstructure in mechanical performance of closed-cell Al-foams. The most famous scaling laws applied for describing mechanical properties and summarized in (Gibson (2000)) were used for comparative analysis. For open-cell foams made of elastic-plastic materials, dimensional arguments give the correlation of plastic collapse stress, σ_{pl}, relative to the yield strength of solid cell edge material, σ_{ys}, *vs*. relative density, ρ/ρ_s , as:

$$\frac{\sigma_{pl}}{\sigma_{ys}} = C_3\left(\frac{\rho}{\rho_s}\right)^n \tag{1}$$

where n=3/2 is power index and the constant C_3 related to cell geometry is roughly about 3.

For closed-cell foams, yielding of stretched cell faces contribute to their strength. Because of this the additional term on right hand side appears in the relation for the plastic collapse stress:

$$\frac{\sigma_{pl}}{\sigma_{ys}} = C_3\left(\frac{\rho}{\rho_s}\right)^n + C_3'\left(\frac{\rho}{\rho_s}\right) \tag{2}$$

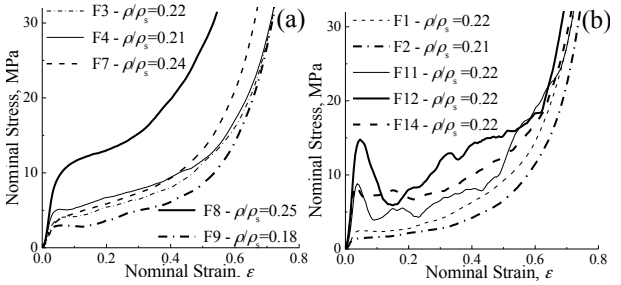

Fig. 2. Compressive stress-strain curves for different Al-foams of comparable relative density, ρ/ρ_s.

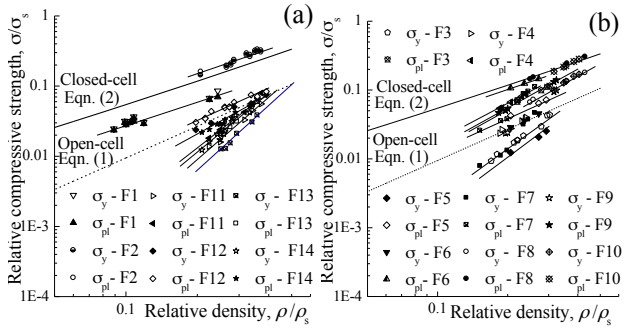

Fig. 3. Relative compressive strength plotted against relative density for different kinds of Al-foams.

where power index n=1.5 and $C_3 \neq C'_3$ are constants.

For tetrakaidecahedral unit with flat faces, finite element analysis gives slightly different values in Eq. 2. Power index at the first term on the right hand side was found as $n = 2$ while the values of constants were determined as great as C_3=0.33 and $C'_3 = 0.44$ (Gibson (2000)).

Generally, compressive strength is usually defined either by "plateau" stress relative to the yield strength or by compressive strength at 20% strain (Gibson (2000)). Both yield stress, σ_y, at the general yielding and plateau stress up to densification, σ_{pl}, (Byakova et al. (2006)) are used in the present study. Approximate values of yield strength, σ_{ys}, for solids compositionally corresponded to the cell wall materials were determined by conventional mechanical tensile tests. The values of parameters σ_{ys} are listed in Table 2.

Following Gibson (2000) data for the relative compression strength, σ_y/σ_{ys} and σ_{pl}/σ_{ys}, of different kinds of Al-foams are plotted in Fig. 3 along the lines representing Eqs. 1 and 2. Fig. 3 (a) shows that the data for carbonate Al-foam F2 lie close to Eq. 2, as prescribed by the theory for closed-cell foams. However, behaviour of all the other kinds of Al-foams deviates more or less from theoretical predictions. Data for Al-foam F1 lie below Eq. 2 and shift to Eq. 1, as can be seen in Fig. 3 (a). Deviation of experimental results from theoretical predictions suggests the decreased contribution of plastic bending to the failure. The same is true for Al-foams F6, F8, F10. Fig. 3 (b) shows that the data for yield stress of those Al-foams lie well below Eq. 2 and shifted to Eq. 1 whereas those for plateau stress lie close to the line representing strength for closed-cell foam. The discrepancy between Eq. 2 and the data for Al foams F3, F4, F5 is the mostly pronounced. Fig. 3 (b) shows that the data for plateau stress of those Al-foams shift essentially below Eq. 2 while the data for yield stress lie either well below or at least along the line representing open-cell foam. Compressive behaviour of Al-foam F7, F9 is very similar to that of Al-foams F3, F5. The noticeable difference is only that the increased thickness of cell walls causes the compressive strength of Al-foams F7, F9 shifts upwards when relative density increases up to $\rho/\rho_s > 0.20$. Fig. 3 (a) shows that Al-foams F11, F12, F13, F14 exhibit the most deflection of the experimental results from theoretical predictions. The data for yield and plateau stresses of Al-foams F11, F13, F14 shift well below the line representing open-cell foam whereas those of Al-foam F12 lie close to Eq. 1.

Generally, one or another scaling low could be adjusted to approximate compressive strength of the each kind of Al-foams, as was recently shown by Byakova et al. (2012). For instance, the compressive strength of Al-foams F1, F2 complies reasonably well with relations prescribed by Eq. 2 for closed-cell structure. However, it is noticeable that the value of the numerical coefficient C'_3 for Al-foam F1 is somewhat reduced compared to that for Al-foam F2. This is usually associated with a contribution of fracture mode in the collapse of deformation bands (Byakova et al. (2012)). The same is true for Al-foams F8, F10. For other kinds of Al-foams (F3, F4, F5, F6, F7, F9), the values of numerical coefficient C'_3 relating to plateau stress are drastically reduced compared to that prescribed by Eq. 2. Moreover, numerical coefficient C'_3 relating to yield stress is completely degraded into zero. The results of approximation show that strength degradation for Al-foams F11, F12, F13, F14 is strong at the most. Besides that the values of numerical coefficient C'_3 relating to yield and plateau stresses are degraded into zero, power index at the first term of Eq. 2 rises up to n=3.

Thus, discrepancies of the actual compressive strength for Al-foams and theoretical predictions reflect the difference in their micro-mechanism of deformation. By considering the evidences above it is easy to show that damage behaviour of the cell wall constituents affects primary micro-mechanism of deformation, favouring either plastic buckling or brittle failure of the cell walls.

In addition, compressive stress, which Al-foams can undergo up to densification, is proved to be actually very sensitive to small defects induced by crushed brittle constituents in the cell wall microstructure.

An attention should be paid to the fact that effect of brittle constituents in the cell wall material on degradation of strength properties is much strong. As it can be seen in Fig. 3, the latter is comparable with that implemented by decreasing a relative density, ρ/ρ_s, of intact Al-foam that is free of defects.

4. Conclusions

By using different kinds of closed-cell Al-foams produced via Alporas like route crucial role of the foaming agent and Ca additive in contamination of the cell wall material by side products and, in turn, macroscopic mechanical response was justified.

Correlations of the relative compressive strength, σ/σ_{ys}, *vs.* relative density ρ/ρ_s, were obtained and analyzed. No discrepancy between experimental values of compressive strengths for Al-foams comprising ductile cell wall constituents and those prescribed by the theoretical models based on an idealized representation of defect free cellular structure for closed-cell structure is found while the opposite was believed to be true in the presence of low ductile and/or brittle processing contaminations including particles/layers of Al_3Ti, residues of partially reacted TiH_2, Ca-bearing compounds and/or modified eutectic domains. The latter contaminations result in reducing the compressive strength to values close to or even below those of open-cell foams of the same relative density, ρ/ρ_s. Considerable discrepancy of actual compressive strength of Al-foams and theoretical predictions was resulted from difference in micro-mechanism of deformation, which, in turn, is affected by damage behavior of the cell wall constituents, favoring either plastic buckling or brittle failure of the cell walls.

The results of this work bring to a better understanding of the interplay between processing conditions, cell wall microstructure, damage behavior of cell wall constituents, and mechanical response of Al-foams.

References

Ashby, M. F., Evans, A. G., Fleck, N. A., Gibson, L. J., Hutchinson, J. W., Wadley, H. N. G., 2000. Metal Foams: A Design Guide, Butterworth Heinemann Press, New Delhi, USA, 251 p.

Byakova, A. V., Gnyloskurenko, S. V., Sirko, A. I., Milman, Y. V., Nakamura, T. 2006. The role of foaming agent in structure and mechanical performance of Al based foams. Materials transactions 47, 2131–2136.

Byakova, A.V., Gnyloskurenko, S.V., Nakamura, T., 2012. The Role of Foaming Agent and Processing Route in the Mechanical Performance of Fabricated Aluminum Foams, Metals 2, 95–112.

Gibson, L.J., 2000. Mechanical behavior of metallic foams, Annual Review of Materials Science 30, 191–227.